In – depth chemical and optoelectronic analysis of triple-cation perovskite thin films by combining XPS profiling and PL Imaging

Stefania Cacovich, Pia Dally, Guillaume Vidon, Marie Legrand, Stéphanie Gbegnon, Jean Rousset, Jean-Baptiste Puel, Jean-François Guillemoles, Philip Schulz, Muriel Bouttemy, et al.

Supporting Information

In – depth chemical and optoelectronic analysis of triple-cation Perovskite thin films by combining XPS profiling and PL Imaging

Stefania Cacovich[†] [(1)], Pia Dally[†] [(2,3)], Guillaume Vidon [(2)], Marie Legrand [(2,4)], Stéphanie Gbegnon [(2)], Jean Rousset [(2,4)], Jean-Baptiste Puel [(2,4)], Jean-François Guillemoles [(1)], Philip Schulz [(1)], Muriel Bouttemy [(2,3)], Arnaud Etcheberry [(3)]

[(1)] CNRS, Institut Photovoltaïque d'Île de France (IPVF), UMR 9006, 18 boulevard Thomas Gobert, 91120, Palaiseau, France

[(2)] Institut Photovoltaïque d'Île de France (IPVF), 18 boulevard Thomas Gobert, 91120, Palaiseau, France

[(3)] Institut Lavoisier de Versailles (ILV), Université de Versailles Saint-Quentin-en-Yvelines, Université Paris-Saclay, CNRS, UMR 8180, 45 avenue des Etats-Unis, 78035 Versailles Cedex, France
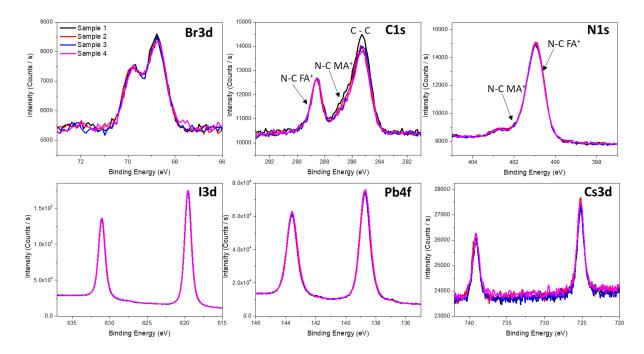
[(4)] EDF R&D, Institut Photovoltaïque d'Île de France (IPVF), 18 boulevard Thomas Gobert, 91120, Palaiseau, France

[†] Equal contribution

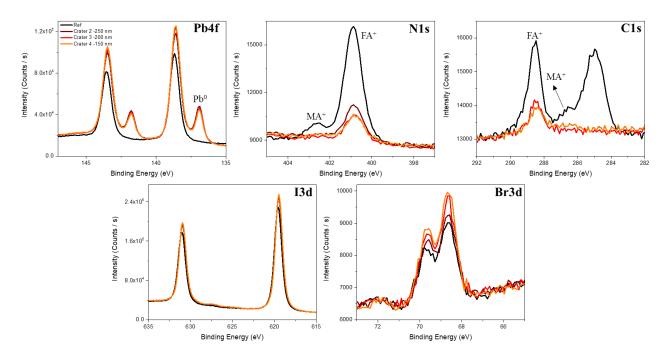Corresponding Author: philip.schulz@cnrs.fr

Figure S1. XPS high-resolution spectra of Br 3d, C 1s, N 1s, I 3d, Pb 4f and Cs 3d for the 4 studied samples. The C – N contribution at 288.3 ± 0.2 eV corresponds to the FA^+ environment and the peak at 286.4 ± 0.2 eV to the MA^+ one. The obtained spectra for the 4 samples are strictly identical, demonstrating identical chemical perovskite atomic network.

Atomic %	Fresh Perovskite	After 1h analysis
$I3d_{5/2}$	30.9	30.7
$Pb4f_{7/2}$	9.5	10.0
N1s	18.7	18.7
$Cs3d_{5/2}$	0.6	0.5
C1s	33.9	33.8
O1s	0.6	0.8
Br3d	5.8	5.7

Table S1. Atomic percentage of $I3d_{5/2}$, $Pb4f_{7/2}$, N1s, $Cs3d_{5/2}$, C1s, O1s and Br3d for fresh Perovskite and after 1h of analysis under X-ray beam.

Crater number	Estimated remaining thickness [nm]	Average Roughness (RMS) [nm]
Surface before sputtering	400	14 ± 2
2	250	17 ± 2
3	200	17 ± 3
4	150	18 ± 3
5	100	16 ± 4
6	Interface perovskite /TiO$_2$	20 ± 5

Table S2. Values of the average roughness measured via Gwyddion software for different estimated thicknesses in the perovskite layer.

Figure S2. XPS high-resolution spectra of Pb 4f, N 1s, C 1s, I 3d and Br 3d, before sputtering (Ref) and after 60 s (crater 2 – 250 nm), 120 s (crater 3 – 200 nm), and 180 s (crater 4 – 150 nm) of sputtering.

TR-PL fitting model

Figure S3: Fitting result of the time resolved measurement. (a-d) Experimental decays at three fluences (4, 10, 30e11 ph.cm^{-2}) overlaid with the fitting model (green dashes). (e) Fitted top surface recombination velocity as a function of the thickness of the Ar etched crater.

Modeling time resolved photoluminescence

The model we used to interpret the decays is the 1d-Drift-Diffusion model. This model is the following. (Ref S1)

We consider a slab of intrinsic semiconductor of thickness L (the thickness is changed in the model for each etching time). The laser pulse will generate excited charges in the device. We consider that the electron and hole density to be equal at all position in the thickness and time. We model the time and space (in thickness) dependent photo generated carrier density $\Delta n(z,t)$ with the 1d-Drift-Diffusion equation:

$$\frac{\partial \Delta n}{\partial t} = D \frac{\partial^2 \Delta n}{\partial z^2} - k_1 \Delta n - k_2 \Delta n^2 + g(z,t) \tag{S1}$$

With the effective diffusion coefficient D, the SRH recombination constant k_1 and the radiative external recombination coefficient k_2. The laser pulse is modeled via the time dependent generation rate g via:

$$g(z,t) = \left[n_\gamma \alpha e^{-\alpha z}\right] \times \left[\frac{1}{\sqrt{2\pi}\sigma} \exp\left(\frac{-t^2}{2\sigma^2}\right)\right]$$

That is Beer-Lambert's absorption law with α the absorption coefficient at the laser wavelength $\alpha(532nm) = 5e4\ cm^{-1}$ and n_γ the fluence in ph.cm^{-2}pulse^{-1} which is varied during the experiment. The right part of g is a Gaussian temporal profile of duration $\sigma = 5ps$ in the simulation.

The boundary conditions to solve Eq S1 are the following:

$$\begin{cases} \left.\dfrac{\partial \Delta n}{\partial z}\right|_{z=0} = S_{top}\Delta n(z = 0, t) \\ \left.\dfrac{\partial \Delta n}{\partial z}\right|_{z=L} = -S_{bot}\Delta n(z = L, t) \end{cases}$$

They represent non-radiative recombination at the interfaces.

The implementation of the model is made via a Matlab code using the pdepe function to solve the partial differential equation. A fitting procedure was coded and has the following properties:

1. A unique model is fitted for all the selected fluences. That means that only one value for the physical parameters is fitted – no fluence dependent values are fitted.

2. The uncertainties on the fitted parameters are estimated using the nlparci method. They are an estimate of the uncertainties – which are difficult to determine for this non-linear fitting method. (Ref S2)

Parameter	Symbol	Value	Comment
Thickness	L	Varied for each set of curves	From the expectation

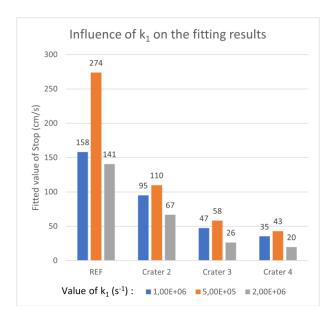|			
Bulk defect SRH coefficient	k_1	$1e6\ s^{-1}$	Estimation from previous knowledge
Radiative recombination coefficient	k_2	$3 \times 10^{-10}\ cm^3 s^{-1}$	Fitted from the full cell reference
Diffusion coefficient	D	$1 \times 10^{-2}\ cm^2 s^{-1}$	From a fit of the thin film reference.
Bottom surface recombination velocity	S_{bot}	$0 cm.\,s^{-1}$	Hypothesis to compare the impact of the top surface
Absorption coefficient at 532nm	$\alpha(532nm)$	$5e4\ cm^{-1}$	Estimated from absorption measurements

Table S3. Model parameters values.

The model parameters are presented in Table S1. We chose to estimate the bulk recombination coefficient k_1 to $10^6\ s^{-1}$ as this value is close to what we found previously for our baseline perovskite.

To analyze the impact of the etching on the recombination, we fitted for each set of curves (a-d of Fig. S2) the drift diffusion model with only one varying parameter: the top surface recombination velocity S_{top}. The results are given in Fig S2 (e). We observe that the top surface recombination velocity is found to decrease with the decreasing thickness. This suggests that the etching did not compromise the quality of the surface. With the fitted parameters, bulk non-radiative recombination account for 22% (400nm-thick device) to 27% (150nm-thick device) of all recombination at 1 sun equivalent illumination, while top-surface recombination account for 77% (400nm-thick device) to 71% (150nm-thick device). The remaining are radiative recombination.

Impact of the value of the parameter k1 on fitting results

To check the influence of the parameter k1 we reperform the fit with different values of k1. The base value was set to k1=1e6 s-1. We test two other values: dividing by two or multiplying by two. We obtain the following fitting results:
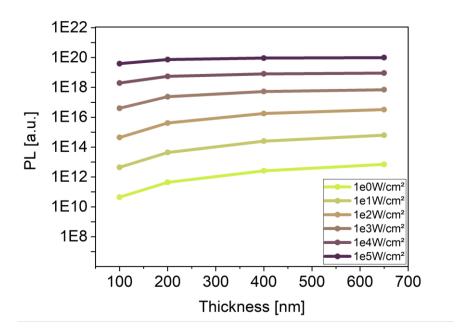

Figure S4: Fitting results with different values of k1 used. Blue corresponds to what is given in the article. Orange is when k1 is divided by two. Grey when k1 is doubled. For all, the uncertainty from the fitting procedure was of the order of 1 cm/s.

We see that some conclusions are true irrespective of the value of k1: the value of the surface recombination parameter decreases for thinner craters. This confirms that the Ar Etching is not causing major damage to the surface recombination in the TR-PL experiment.
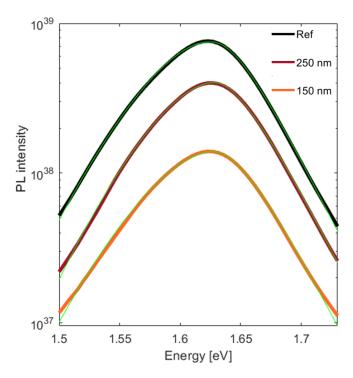
When the value of k1 is reduced (orange bars), the surface recombination is increased which is coherent: the model needs to have a certain amount of non-radiative recombination that can either come from the surface or the bulk of the material. As we mentioned in the main text, this makes that the parameters k1 and Stop are highly anti correlated. In [3], Hutter et al explain how TR-PL is a powerful tool but cannot distinguish different sources of non-radiative recombination one from the other. That is why we choose to fix the value of k1 and to interpret the variations of non-radiative recombination in terms of surface recombination.

7

Modeling the effect of thickness on PL peak

In order to decorrelate the effect of thickness and potential surface modification on steady-state hyperspectral PL acquisitions, we performed drift-diffusion simulation with Atlas solver. We modelled the effect of thickness decrease keeping material properties constant in order to conclude on its impact on PL. We observed in **Figure S3** that when the thickness is decreased, the PL peak decreases which is in agreement with the observed analysis. When the thickness decreases, the surface recombination exhibits a more significant effect. The surface/volume ratio increases which leads to a decrease in bulk recombination versus surface recombination. Complementary experimental analysis detailed in the main section of the manuscript aids in deducing whether the thickness is the only factor impacting the PL peak intensity decrease or if the surface recombination is changed at the same time.
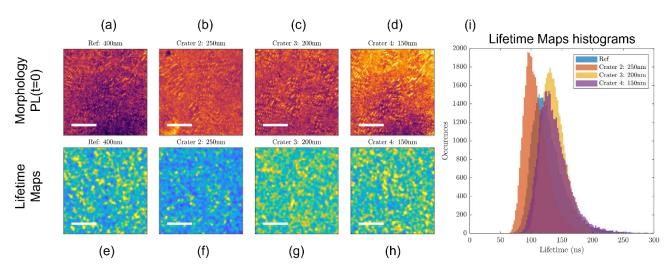

Figure S5. Influence of the perovskite thin film thickness on the maximum PL intensity. The incident illumination power was varied from 1 W/cm^2 to 1e5 W/cm^2.
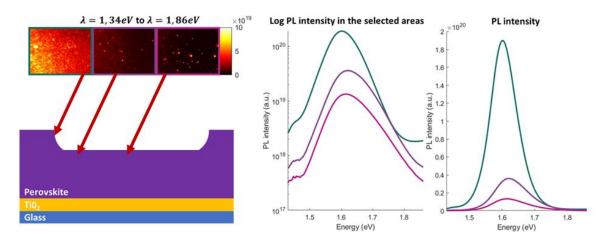
Figure S6. PL average spectra and corresponding fitting curve for reference sample, crater 2 and crater 4. The model used for the fitting is based on Planck's law as described in the main text.

Comparison of morphology and lifetime maps

Figure S7: (a-d) Maps of the average PL signal between t=0 and t=3ns for each of the samples. (e-h) Lifetime maps as shown in the main article. (i) Histogram of the lifetime maps values.

Figure S8: Hyperspectral acquisition in different location of the crater. (left) Corresponding PL intensity maps. (right) Spectra of the different acquisitions

References

1) Maiberg, M., & Scheer, R. (2014). Theoretical study of time-resolved luminescence in semiconductors. II. Pulsed excitation. Journal of Applied Physics, 116(12), 123711.
2) Young, P. (2015). Everything You Wanted to Know About Data Analysis and Fitting but Were Afraid to Ask. Springer International Publishing. https://doi.org/10.1007/978-3-319-19051-8
3) Hutter, E. M., Kirchartz, T., Ehrler, B., Cahen, D., & Hauff, E. von. (2020). Pitfalls and prospects of optical spectroscopy to characterize perovskite-transport layer interfaces. *Applied Physics Letters*, *116*(10), 100501. https://doi.org/10.1063/1.5143121